Proteomic Analysis of Ethanol Reduced Susceptibility Mutants

By

HADASSAH MARQUART

A Thesis submitted to the Honor's College

In partial fulfillment of an Honor's Bachelor's degree in

Biochemistry and Molecular Biology

Oklahoma State University

May 2020

Table of Contents

Abstract

Staphylococcus aureus are dangerous pathogens responsible for thousands of deaths every year, and it is estimated that 95 million Americans may be carriers of a *S. aureus* strain (1). Even more dangerous is the subset of Multiple Resistant *Staphylococcus aureus* (MRSA). MRSA commonly cause nosocomial infections, but the prevalence of MRSA in the community is increasing. The use of alcohol-based hand rubs (ABHR) has greatly increased hand hygiene compliance and convenience to combat hand carriage of *S. aureus*. To study the effects of alcohol as a selective pressure on the bacteria, the Gustafson laboratory passaged Methicillin susceptible *S. aureus* strain SH1000 through up to 12% ethanol and conducted proteomic analysis of isolated ethanol reduced susceptibility SH1000 mutants SH123 and SH124. Concentrations of proteins associated with multiple notable systems were found altered: iron acquisition and autolysis proteins were increased, while proteins associated with purine biosynthesis, virulence, and an alcohol dehydrogenase were present in decreased concentrations in the mutants. Autolysins may function to remove peptidoglycan damaged by ethanol during exposure to the biocide. I hypothesize that the increased autolysin concentrations in the mutants are leading to iron leakage secondary to cell wall breakdown, resulting in increased need for siderophores and iron transporters. In addition, I hypothesize that the decrease of other system proteins is explained by the slow growth phenotype resulting in a lower energy demand and conservation of resources through reducing non-vital functions.

Introduction

Multidrug-resistant *Staphylococcus aureus* (MRSA) such as methicillin-resistant *S. aureus* were responsible for 19,832 associated deaths in the United States alone in 2017: this is

much higher mortality than human immunodeficiency virus (HIV), which caused 5,698 deaths in the same timeframe (2, 3). This bacterium is spread from person to person in large part via hand carriage. For this reason, hand antisepsis is incredibly important to prevent infections caused by *S. aureus*, especially in nosocomial environments (4). There are a number of methods available to reduce hand carriage of bacteria, but the use of alcohol based hand rubs (ABHR) is very effective and has increased hand antisepsis compliance through ease of use (5-7).

To test for possible growing tolerance of *S. aureus* to the alcohols used in ABHR, laboratory parent strain SH1000 was passaged through increasing concentrations of ethanol up to 12%. Ethanol reduced susceptibility *S. aureus* SH1000 mutants were then isolated from the final cultures containing 12% ethanol (8, 9). These colonies display a small colony variant phenotype, which are significantly smaller in size compared to the parent SH1000 and slow growing (8, 10). Small colony variants are often associated with recurring infections as they are overall less susceptible to antimicrobial therapy (11).

Proteomic analysis of two of the isolated ethanol reduced susceptibility (ERS) SH1000 mutants, SH123 and SH124, revealed increased concentrations of multiple autolysin proteins and iron-acquiring staphyloferrin proteins compared to the parent SH1000, as well as increased iron transport proteins, multiple decreased purine metabolism proteins, and decreased virulence factors (12). The increased concentration of autolysins may indicate a cause of the apparent iron starvation: if increased autolysin activity is making the peptidoglycan layer more permeable, iron may be escaping the cell via the damaged cell wall. This review examines the functions and synthesis of the proteins involved in order to support the stated hypothesis and outline future testing, as well as analyze altered concentrations of other proteins within the ERS mutants.

Materials & Methods

Ethanol Passaging & Mutant Selection

To test *S. aureus* growth under the selective pressure of ethanol, laboratory strain SH1000 was passaged through increasing concentrations of ethanol before mutants were selected. Among 106 MRSA strains investigated, the most common minimum inhibitory concentration (MIC) of ethanol was 9% v/v (13). As such, 9% v/v was chosen as the starting concentration of ethanol in the passaging. Ethanol was sterilized with a 0.2 um nylon filter before being added to Mueller-Hinton broth (MHB) (14).

Overnight cultures of SH1000 were used in 2% v/v inoculation of MHB containing the initial 9% ethanol v/v. This culture was incubated at 37°C shaken at 200rpm until visually turbid. A 2% inoculum of this initial culture was then added again to fresh MHB containing 9% ethanol and incubated (14). This was repeated until the fifth 9% culture, which was used to inoculate a 10% ethanol v/v media. In this way, the SH1000 was grown 5 times at each concentration of ethanol before being moved to a 1% v/v higher concentration. Media with ethanol concentrations of 9%, 10%, 11%, and 12% were used. The entire passaging process of SH1000 took 55 days to complete (14).

At the fifth passage at 12% ethanol v/v, one loopful of liquid culture was used to inoculate a drug free Mueller-Hinton Agar (MHA) plate. From the growth on the MHA plate, 5 random colonies were selected and named SH1000 mutants SH121 through SH125. The mutants were plated onto further MHA plates, and passaged with the solid media. The third MHA plate from each mutant was used to prepare frozen stock cultures (14).

Collection & Analysis of Proteomic Data

Cells were lysed with polymer beads to collect cell proteins for each strain under study. Proteins were precipitated out, then digested with trypsin before running mass spectrometry (MS). Specifically, liquid chromatography and tandem mass spectroscopy (LC-MS/MS) was used (15, 16). The digested peptides were first run through a 2.5cm protective guard column to remove possible contaminants and improve performance of the main analytical column. The analytical column used was 15cm long with an internal diameter of 75μm, ending in a fused silica emitter for the nanoelectrospray ion source (16). Upon exiting the analytical column, the eluate was ionized by the emitter for analysis by the mass spectrophotometer. By analyzing the mass to charge ratios of the ionized peptides, the mass spectrophotometer produced a graph used to identify the amino acids in the peptide fragment. The Andromeda peptide search engine with MaxQuant was used to compare these resulting MS data to a database of proteins from *S. aureus* strain NCTC 8325, ID9306, which was downloaded from UniProt (15). Protein concentrations were determined through the peak intensity of the MS data, using the LFQ algorithm within MaxQuant (16). The gene loci provided by Andromeda were then analyzed manually through PubMed Protein BLAST search and STRING database to further identify genes and proteins.

Autolysis experiment

Performance of an autolysis assay will help determine what effect the increased concentrations of autolysin proteins have on cell wall degradation in our isolated ERS mutants SH123 and SH124. Supported by the findings of Bose, Lehman, Fey, and Bayles (2012), we expect increased rates of autolysis in our mutants in comparison to the parent strain (17). In this previous study, it was determined that the deletion of the *atl* gene resulted in dramatic loss of autolysis in *S. aureus* in the stationary phase (17). If this is the case, it would support our

hypothesis that increased autolysin concentrations in ERS mutants SH123 and SH124 are disrupting the integrity of the cell wall leading to leakage of cell contents, specifically iron.

A 1% inoculum of overnight bacterial culture of each strain being tested, mutants SH123 and SH124 in addition to parent SH1000, was added to 30mL of LB broth in a growth flask and allowed to grow to an OD_{580nm} of 0.7 at 37°C with shaking. This was used as the base culture from which we performed the autolysis. Twenty-five mL of this culture was centrifuged, and the pellet washed with 5mL of sterile ice-cold water. The cell pellet was resuspended in 25mL of 0.05M Tris buffer solution with 0.05% Triton X100 detergent in a 25mL growth flask. The flask was incubated at 37°C with gentle agitation: OD_{580} was read every 30 min for the following 6 h. Due to the small colony variant trait of extremely slow growth in mutants SH123 and SH124, overnight cultures were incubated for two days rather than one, and the growth phase preceding the autolysis experiment required more time than the parent to reach OD_{580nm} 0.7.

During attempt to complete an autolysis assay, both mutant SH123 and SH124 experienced reversion from the slow growing small colony phenotype. We rejected this assay without finishing all 6 hrs of measurements, as there was no way to effectively verify this was not a new and separate mutation that would genetically separate these cells from either SH123 or SH124 mutant cells. Repetition of the attempt was not completed due to extenuating circumstances.

Results & Discussion

Proteomic Data

Mutants SH123 and SH124 both showed significant deviation from SH1000 in regards to several protein concentrations. Significance of altered protein concentrations is defined using a p value of 0.05 with results measured on a log2 scale. A value of 1 indicates the protein is present in the mutant at double the concentration found in SH1000. In mutant SH123, 160 proteins differed from SH1000 in concentration, of which 62 were increased. In mutant SH124, there were 126 altered concentration proteins, with 45 of these increased (12). Shown below in Table 1 are only those proteins whose concentrations were significantly altered in both SH123 and SH124 (12). Proteins of interest to be discussed have been marked in bold.

Table 1: Proteins Differentially Expressed in Both SH123 and SH124

SH123vsSH1000 log2(ratio)	SH124vsSH1000 log2(ratio)	Protein Name	Gene Locus	Protein Function
5.358	**4.705**	**SbnF**	**SAOUHSC_00080**	**3-(L-alanin-3-ylcarbamoyl)-2-[(2-aminoethylcarbamoyl)methyl]-2- hydroxypropanoate synthase**
5.279	**4.509**	**SbnE**	**SAOUHSC_00079**	**L-2,3-diaminopropanoate--citrate ligase**
4.603	**4.157**	**SbnH**	**SAOUHSC_00082**	**staphyloferrin B biosynthesis decarboxylase**
4.379	**3.894**	**SbnI**	**SAOUHSC_00083**	**bifunctional transcriptional regulator/O-phospho-L-serine synthase**
4.351	**3.615**	**SbnB**	**SAOUHSC_00076**	**N-((2S)-2-amino-2-carboxyethyl)-L-glutamate dehydrogenase;**
4.317	**3.568**	**LytM**	**SAOUHSC_00248**	**Glycine-glycine endopeptidase**
4.245	**3.445**	**SceD**	**SAOUHSC_02333**	**transglycosylase SceD**
3.564	**2.938**	**SbnG**	**SAOUHSC_00081**	**Siderophore biosynthesis protein**
3.458	1.620	ClfA	SAOUHSC_00812	Clumping factor A
2.818	1.087	*sdaAB*	SAOUHSC_02840	**L-serine ammonia-lyase, iron-sulfur-dependent, subunit beta**
2.653	**1.694**	**SbnC**	**SAOUHSC_00077**	**staphyloferrin B biosynthesis protein**
2.479	1.984	BetA	SAOUHSC_02932	Choline dehydrogenase
2.254	2.420	BetB	SAOUHSC_02933	Betaine aldehyde dehydrogenase
2.194	1.173		SAOUHSC_01062	DUF1506 family protein
2.170	1.309		SAOUHSC_00811	uncharacterized N-acetyltransferase
2.039	**1.597**	**Atl**	**SAOUHSC_00994**	**Bifunctional autolysin precursor**
1.904	**1.675**	**FecCD region°**	**SAOUHSC_02428**	**iron ABC transporter permease**
1.839	1.421	YlmE	SAOUHSC_01153	Pyridoxal phosphate dependent enzyme
1.770	1.469		SAOUHSC_01584	DU1672 domain containing protein
1.715	1.628	YlmH	SAOUHSC_01156	uncharacterized RNA-binding protein
1.665	1.545		SAOUHSC_01413	Mox family ATPase
1.637	**1.775**	**SfaA**	**SAOUHSC_02433**	**Staphyloferrin A biosynthesis protein**
1.334	1.909	CbdA	SAOUHSC_01031	**Cytochrome d ubiquinol oxidase, subunit I**
1.299	1.336		SAOUHSC_02296	SprT family protein
1.276	1.592		SAOUHSC_00523	Class I SAM-dependent methyltransferase
1.259	1.182		SAOUHSC_01660	Nif3-like dinuclear metal center hexameric protein
1.202	1.795		SAOUHSC_02905	DUF4176 domain-containing protein
1.187	1.108		SAOUHSC_01661	tRNA (adenine-N(1))-methyltransferase
1.182	1.485		SAOUHSC_02668	DUF3139 domain-containing protein
1.130	1.043		SAOUHSC_02458	DUF3885 domain-containing protein
1.105	**1.212**	**fhuG**	**SAOUHSC_00654**	**iron ABC transporter permease**
1.091	1.545		SAOUHSC_01650	5-formyltetrahydrofolate cyclo-ligase
1.046	2.167	YlmG	SAOUHSC_01155	YggT family protein
-1.031	-1.046		SAOUHSC_00501	NupC/NupG family nucleoside CNT transporter
-1.037	-1.251	atpC	SAOUHSC_02340	**F0F1 ATP synthase subunit epsilon**
-1.174	-1.055		SAOUHSC_01320	homoserine dehydrogenase
-1.190	-1.245	HsdR	SAOUHSC_00162	type 1 restriction endonuclease subunit R
-1.193	-1.292	queH	SAOUHSC_02911	Epoxyqueuosine reductase QueH
-1.211	-1.169		SAOUHSC_02129	staphostatin A
-1.213	-1.299		SAOUHSC_00844	MetQ/NlpA family ABC transporter substrate-binding protein
-1.228	**-1.373**	**cvfC**	**SAOUHSC_01437**	**Conserved virulence factor C**
-1.243	-1.143	radA	SAOUHSC_00507	DNA repair protein
-1.278	-2.029	*pycA*	SAOUHSC_01064	Pyruvate carboxylase
-1.284	-1.101	YgiL	SAOUHSC_00336	acetyl-CoA C-acetyltransferase
-1.290	-1.609		SAOUHSC_00357	helix-turn-helix transcriptional regulator
-1.296	-1.348	BstA	SAOUHSC_03028	bacillithiol transferase

-1.299	-1.569	Ldh2	SAOUHSC_02922	L-lactate dehydrogenase 2
-1.316	-1.348	hutH	SAOUHSC_00008	Histidine ammonia-lyase
-1.424	**-2.002**	**adhP**	**SAOUHSC_00608**	**Alcohol dehydrogenase**
-1.467	-1.981		SAOUHSC_00209	PTS glucose transporter subunit IIB
-1.482	-1.981		SAOUHSC_02582	formate dehydrogenase subunit alpha
-1.508	-1.622	glcB	SAOUHSC_02848	glucoside-specific EIICBA component
-1.518	-3.389	argG	SAOUHSC_00899	Argininosuccinate synthase
-1.524	-1.455	AdcA	SAOUHSC_02690	Zinc ABC transporter substrate-binding lipoprotein
-1.603	**-1.081**	**guaC**	**SAOUHSC_01330**	**GMP reductase**
-1.607	-1.311		SAOUHSC_01920	>tr|Q2G2Y5|Q2G2Y5_STAA8 Uncharacterized protein OS=Staphylococcus aureus (strain NCTC 8325) OX=93061 GN=SAOUHSC_01920 PE=4 SV=1
-1.633	**-2.473**	**sbi**	**SAOUHSC_02706**	**Immunoglobulin-binding protein sbi**
-1.656	-1.918	azoR	SAOUHSC_00173	FMN-dependent NADH-azoreductase
-1.662	-1.249		SAOUHSC_02829	NAD(P)H oxidoreductase
-1.695	-1.385		SAOUHSC_00430	GNAT family N-acetyltransferase
-1.710	-1.721		SAOUHSC_01729	>tr|Q2FXV2|Q2FXV2_STAA8 Uncharacterized protein OS=Staphylococcus aureus (strain NCTC 8325) OX=93061 GN=SAOUHSC_01729 PE=4 SV=1
-1.722	-2.050	metN2	SAOUHSC_00842	Methionine ABC transporter ATP-binding protein
-1.768	**-1.501**	**purD**	**SAOUHSC_01018**	**Phosphoribosylamine--glycine ligase**
-1.800	-1.920		SAOUHSC_02597	PTS alpha-glucoside transporter subuit IIBC
-1.898	**-2.266**	**purM**	**SAOUHSC_01015**	**Phosphoribosylformylglycinamidine cyclo-ligase**
-1.907	-4.132	stpC	SAOUHSC_02820	ATP-binding cassette domain-containing protein
-1.917	-1.564		SAOUHSC_00164	sce7725 family protein
-1.931	-1.294		SAOUHSC_00200	Putative membrane protein
-1.985	-2.203		SAOUHSC_02393	SAP domain-containing protein
-2.094	**-1.779**	**purH**	**SAOUHSC_01017**	**bifunctioning phosphoribosylaminoimidazolecarboximide formyltransferase/IMP cyclohydrolase**
-2.105	-2.088		SAOUHSC_02648	L-lactate permease
-2.143	**-2.552**	**sarS**	**SAOUHSC_00070**	**HTH-type transcriptional regulator SarS**
-2.226	-2.905	pflB	SAOUHSC_00187	Formate C-acetyltransferase
-2.267	-1.254		SAOUHSC_00711	HlyC/CorC family transporter
-2.359	**-1.147**	**purE**	**SAOUHSC_01008**	**5-(carboxyamino)imidizole ribonucleotide mutase**
-2.554	**-1.780**	**purC**	**SAOUHSC_01010**	**Phosphoribosylaminoimidazole-succinocarboxamide synthase**
-2.665	-3.312		SAOUHSC_00717	DM13 domain-containing protein
-2.747	-1.722		SAOUHSC_00738	peptide MFS transporter
-2.863	-3.233	sarZ	SAOUHSC_02669	HTH-type transcriptional regulator SarZ
-3.304	-2.289	tagB	SAOUHSC_00222	CDP-glycerol glycerophosphotransferase family protein
-3.631	**-2.147**	**purK**	**SAOUHSC_01009**	**5-(carboxyamino)imidizole ribonucleotide synthase**
-3.725	-2.412		SAOUHSC_00410	GTP binding protein
-3.868	-3.757		SAOUHSC_01110	Fibrinogen-binding protein
-5.123	**-3.329**	**purQ**	**SAOUHSC_01012**	**Phosphoribosylformylglycinamidine synthase subunit**
-6.313	**-2.891**	**sdrD**	**SAOUHSC_00545**	**MSCRAMM family adhesin SdrD**
-9.377	**-7.151**	**spA**	**SAOUHSC_00069**	**Immunoglobulin G-binding protein A**

°This protein is unknown, but contains an FECCD region

Autolysins

Autolysins break down the wall of the bacteria producing the protein. Despite the inherent risk of a cell degrading its own outer protective coating of peptidoglycan, autolysins are necessary to allow for cell growth, division, and separation, as well as cell wall turnover: it seems almost all bacteria have autolysins (18). Without them, the cell wall would be too rigid to allow changes necessary for the cell to grow and reproduce, while damages to the cell wall would be irreparable and could contribute to cell death (18). In the isolated ERS SH1000 mutants, three different autolysin proteins are present in increased concentrations compared to SH1000: SceD, LytM, and Atl (12). Each of these proteins degrades different linkages in the peptidoglycan wall, as visualized in Fig 1 (19). As the exact method through which ethanol kill bacterial cells is poorly understood, any or all of these autolysins may contribute to breaking down peptidoglycan damaged through interaction with biocidal ethanol.

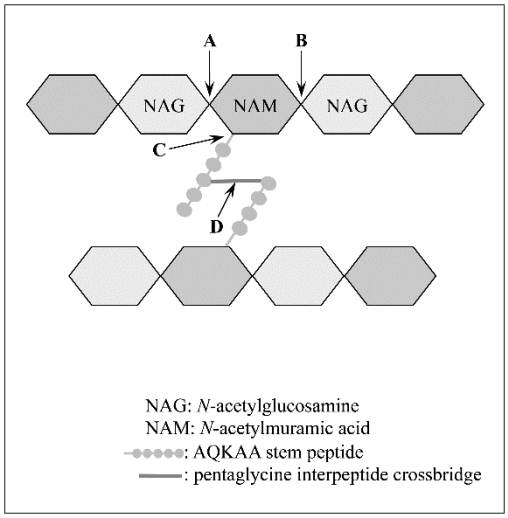

Figure 1:Diagram of S. aureus peptidoglycan and cleavage sites for cell wall hydrolases. A) glycan strand glycosidic bond (glucosaminidase: AtlA). B) glycan strand glycosidic bond (lytic transglycosylases: SceD). C) N-Acetylmuramyl-L-alanyl amide bond (AtlA amidase domain). D) pentaglycine bridge glycyl-glycyl bond (LytM endopeptidase)

SceD is a lytic transglycosylase that breaks the β-1,4 glycosidic bond between NAM and NAG residues at the location indicated by position B in the figure. When inactivated, cell separation is impaired and larger clumps of cells are seen compared to normal growth (18, 20).

LytM is a glycyl-glycyl endopeptidase, hydrolyzing the peptide bond between adjacent glycine residues forming the cross bridges between peptide chains as seen at position D in the Fig 1 (19, 20). Results found by Lioliou et al (2016) indicate that failure to properly regulate

LytM production contributes to perturbation of the cell wall, which could lead to affected cell wall synthesis by affecting binding and transport of modifying enzymes and availability of necessary precursors for cell wall synthesis (21). While unconfirmed, it would follow that LytM may have a negative effect on the fortitude of cell walls within mutants overexpressing the protein and could very well contribute to cell wall permeability resulting in nutrient loss.

The final discussed autolysin, Atl, is recognized as the major autolysin present in *S. aureus* (22). Interestingly the AtlA protein is broken into two autolysin enzymes rather than functioning as one. Point A in Fig 1 illustrates the site of cleavage for the glucosaminidase enzyme: the reaction catalyzed is the hydrolysis of the bond linking a NAG and NAM segment within the peptidoglycan backbone. The second segment functions as an amidase which breaks the bond between a NAM molecule and the alanine residue at the start of the attached peptide chain. This bond is illustrated as point C in the Fig 1 (17, 19). Collectively, the enzymes of AtlA are crucial to proper cell separation during binary fission of S. aureus, and are suspected to degrade the cell wall of the septum connecting daughter cells (17, 20). Deletion of the *atlA* gene in mutants resulted in improper clumping patterns of mutant cells, as daughter cells were incompletely separated (22). Groups of clusters averaging 32 cells each could be found, rather than the typical four or eight cell clusters of *S. aureus*. Additionally, mutants with a a*tlA* deletion revealed a dramatic decrease of cell lysis during the stationary phase (22). As our isolated mutants displayed an increase in Atl concentration, cell autolysis should be increased.

Staphyloferrins and Iron Uptake

The ability to acquire iron is a vital function for all forms of life. Iron is a key element in many metabolic functions including redox reactions, oxidative phosphorylation, and cytochrome complexes in the electron transport chain (23). Additionally, multiple DNA synthesis and repair

proteins, including helicases, nucleases, and demethylases, require iron for proper function. (24). While iron must be tightly regulated to prevent oxidation that could be harmful to a cell, iron also takes a role in protection against reactive oxygen species in a superoxide dismutase (25). However, iron is not always easy to obtain, especially for pathogens in low iron environments. In the body of a host organism, such as humans, free iron is limited by complexing with storage and transport proteins both to prevent oxidative damage and as a function of innate immunity to reduce iron available to possible invaders. A successful pathogen must be able to acquire iron from these host proteins, such as transferrin and hemoglobin, to supply its own needs and survive. One method of pathogenic iron theft is through iron chelators known as siderophores. The iron affinity in these relatively small proteins is higher than that of the host proteins, which allows iron theft by the pathogen (23, 26-29). As these proteins are secreted, the invading bacteria must also have a method of returning the iron to the cell, which is accomplished through active transport.

In the staphylococci, two carboxylate-type siderophores have been extensively defined: staphyloferrins A and B (26, 30-32). Interestingly, both proteins were increased in concentrations in ERS mutants SH123 and SH124 compared to SH1000 (12). Of the two, staphyloferrin A was increased less in relative concentration in the SH123 and SH124 proteomes. In an experiment testing the production of staphyloferrin A in thirty-seven *Staphylococcus* strains, thirty-four strains produced the siderophore when supplemented with D-ornithine, and eleven of these still produced without supplementation (28). Three were S. aureus strains. Staphyloferrin A takes the form of a molecule of D-ornithine linking two molecules of

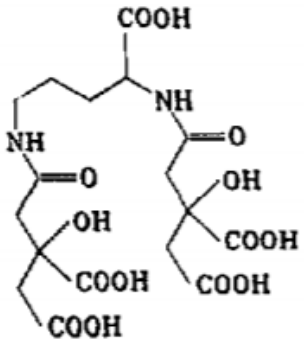

Figure 2: Structure of Staphyloferrin A

citric acid via amide bonds (Fig 2)(28). Within S. aureus, biosynthesis of staphyloferrin A is coded for by the *sfa* operon, which consists of genes *sfaA-D*, of which only *sfaA* was upregulated (Fig 3) (12, 30, 31). After acquiring iron from outside the bacterial cell, staphyloferrin A is returned through the HtsABC transporter system (31). HtsA represents the receptor for the ferric staphyloferrin A protein, while HtsB and HtsC are permeases (31).

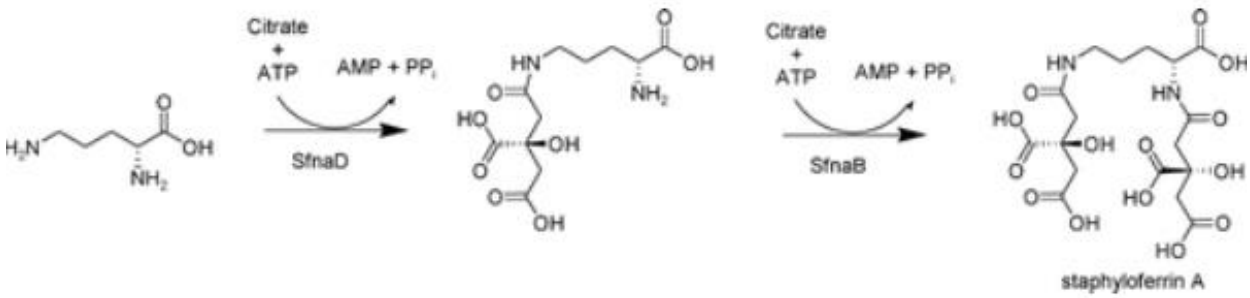

Figure 3: Biosynthesis of Staphyloferrin A. Sfna is an alternate naming system of the sfa genes, as acknowledged by Crigg et. al

Staphyloferrin B was more dramatically increased in relative protein concentration in our analysis, and also appears to be the more commonly produced in the *S. aureus* species. In the previously mentioned study of thirty-seven *Staphylococcus* strains, sixteen produced staphyloferrin B without D-ornithine supplement, including eight of the nine tested *S. aureus* strains (12, 28). Staphyloferrin B biosynthesis is accomplished through a multistep process combining l-2,3-diaminopropionic acid, citric acid, 1,2-diaminoethane, and α-ketoglutaric acid (Fig 4-5) (32). This composition explains the relatively ineffective results of stimulating staphyloferrin B production through D-ornithine supplement. Staphyloferrin B biosynthesis is controlled by nine genes on the *sbn* operon, named *sbnA-I*. Of the top eleven most increased protein concentrations between SH1000 and the

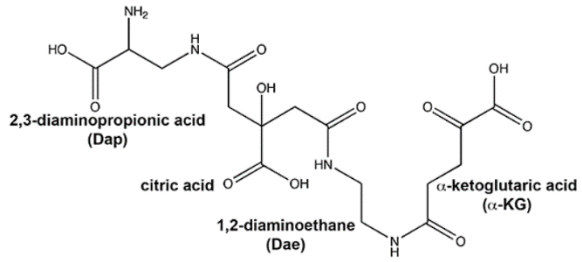

Figure 4: Structure of Staphyloferrin B

isolated mutants, seven were staphyloferrin B biosynthesis proteins: SbnB, SbnC, SbnE, SbnF, SbnG, SbnH, SbnI. Only SbnA and SbnD were not present in increased concentrations within the Sh 123 and SH124 proteomes (12). When returning to the cell, ferric staphyloferrin B is imported via the SirABC transport system (31). SirA receives the siderophore, in association with permeases SirB and SirC (31).

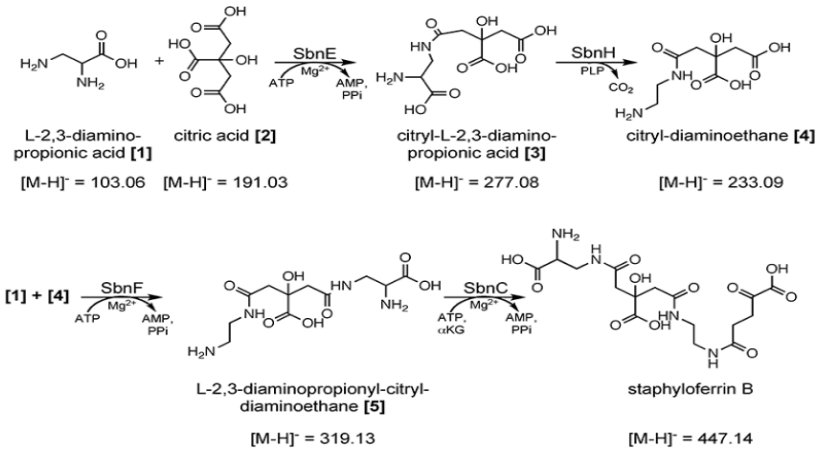

Figure 5: Staphyloferrin B biosynthesis

Staphyloferrins are not the only strategy employed by *S. aureus* to intake additional iron from the extracellular space, however. Two iron ABC transporter permease proteins are increased in concentration as well as staphyloferrins A and B, despite their functions being distinct from that of the staphyloferrins. FhuG is a transporter of Iron (III)-hydroxamate complexes (33). Part of the *fhuCBG* operon, the protein FhuG is critical to the active transport of hydroxamate siderophores such as ferrichrome, aerobactin, and desferrioxamine. Note that staphyloferrins are carboxylate-type siderophores. In fact, current research suggests that *S. aureus* cannot produce hydroxamate siderophores, but can import iron (III)-hydroxamate complexes resulting from the production from other organisms (33). The second iron ABC transporter permease protein is unknown, except that it contains a FecCD region. In a variety of bacteria, FecCD regions are found to be involved in transport of heme-iron complexes, Iron(III)

dicitrate, as well as Iron (III)-hydroxamate, ferric anguibactin, and petrobactin siderophores (34). This consistent function highlights the association of FecCD regions with iron transport. Our unknown protein may be a part of a separate iron transport system, or may very well be another piece of the system in part with our known protein FhuG. Either way our proteomic data clearly shows that at least two different iron acquisition systems are produced in increased concentration in our ERS SH1000 mutants. The ERS mutant cells may have an increased iron requirement in order to combat ethanol stress. Ethanol has been shown to increase production of reactive oxygen species which can damage DNA and reduce the amount of ATP a cell is able to produce, among other negative effects (35). Iron could have a hand in mitigating each of these problems, explaining an acquisition of mutations leading to increased iron demand. Alternatively, the increased concentrations of iron acquisition proteins may indicate iron starvation within SH123 and SH124, which could be explained by the increased concentration of autolysins discussed above.

Alcohol Dehydrogenase

Alcohol dehydrogenase AdhP acts as an oxidoreductase with the help of NAD+/NADH. A primary alcohol is combined with NAD+, resulting in an aldehyde and NADH after catalysis by the two $Zinc^{2+}$ atoms bound within the enzyme (36). Considering SH123 and SH124 were clearly stressed when passaging in high concentrations of ethanol, it seems strange that this dehydrogenase would appear in lower relative concentrations compared to parent strain SH1000. One would expect stress via alcohol to result in increased expression of enzymes that can break down the offending biocide. However, AdhP specifically may be of little use here, as it acts preferentially towards 1-propanol (36, 37). Even if some activity against ethanol is present, it does not seem to be beneficial enough to warrant increased production of the enzyme. While the

AdhP concentration is decreased, other methods are likely being used in an effort to withstand the ethanol stress.

Purine Biosynthesis

In connection with the slow growth of SH123 and Sh124, purine biosynthesis proteins are also displaying markedly lower concentrations compared to SH1000. GMP reductase, coded by gene *guaC*, is decreased in the proteomes of SH123 and SH124. GMP reductase deaminates GMP into IMP with the reducing power of NADPH. In a normal cell, IMP is used as a precursor to either GMP or AMP nucleotides. By reverting a GMP nucleotide back to IMP, it can then be converted to AMP as part of the purine salvage pathway (38, 39). Multiple proteins expressed from the *pur* operon are also decreased: PurC, PurD, PurE, PurH, PurK, PurM, and PurQ. Similar to guaC, the *pur* genes also function to form IMP. Five-phosphoribosypyrophosphate (PRPP) is the main precursor to IMP formation in this pathway, which undergoes a long multi-

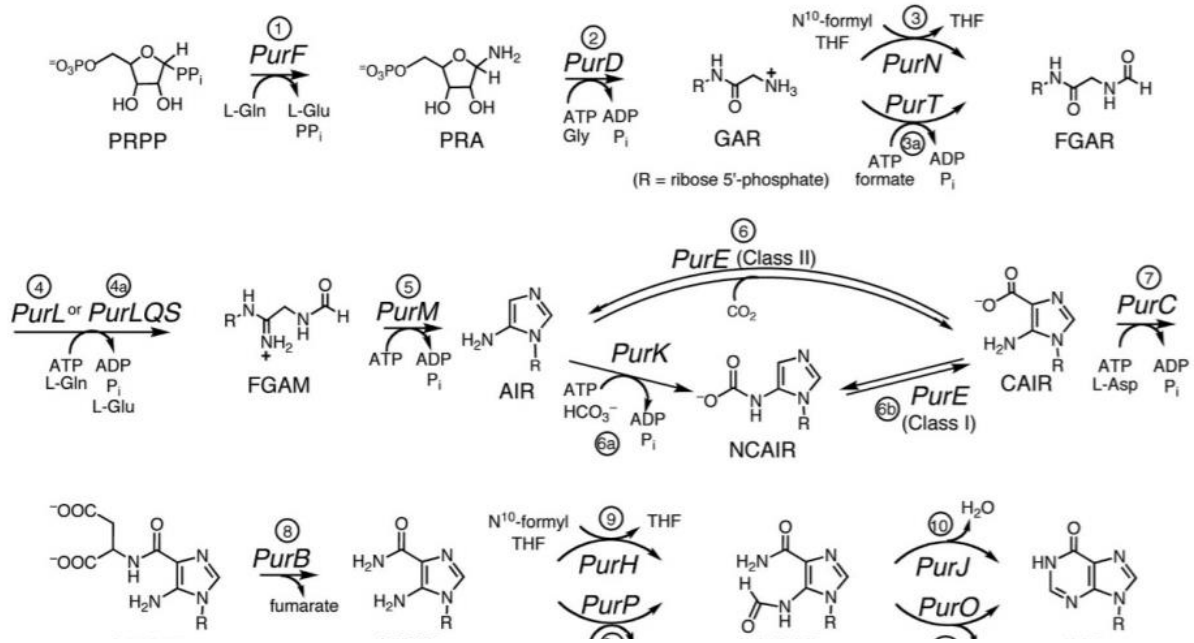

Figure 6: Purine biosynthesis pathway. In our isolated mutants, purCDEHKMQ are present in reduced concentrations

step process to form the nucleotide (40). The main synthetic process is illustrated (Fig 6). Some Pur proteins are only present in certain organisms.

GMP reductase and the *pur* genes both provide mechanisms for IMP production, which serves as a precursor to nucleotide triphosphates ATP and GTP. In the slow growing mutants, the need for purines destined for nucleic acid synthesis is limited, as slow growth and cell division limits the need for DNA replication. This reduced growth and replication reduces energy demand resulting in decreased need of purine energy sources. Proteins within these mechanisms are produced in lower concentrations compared to parent strain SH1000 as a reflection of this lower need. In essence, ERS mutants SH123 and SH124 are at least partially disabling their ability to make ATP.

Virulence

By far the protein group with the most decreased concentrations was virulence factors. In a state of self-preservation, it appears that these cells are functioning with only a "skeleton crew" of metabolic processes necessary for survival. In the research of Pando et al (2017), it was found that *S. aureus* cells under stress by 10% ethanol challenge developed increased expression of proteins needed for persistence and defense of cellular proteins, while decreasing transcription and translation (13). While the cells directly under analysis have not been in contact with ethanol, they are the progeny of the cells isolated from the 12% ethanol media and display the same phenotype as those isolates. Decreased expression of virulence factors may be a part of the limiting of non-vital cell functions that appears to be occurring in these cells. Included among the decreased virulence factors are: SpA, SdrD, Sbi, CvfC, and an unknown fibrinogen bonding protein (12). The decrease in SpaA virulence factor is likely connected to the also decreased SarS, a *S. aureus* sarA homologue that acts as a promoter to Spa (41). SpaA as well as Sbi are

virulence factors known to bind immunoglobulin IgG, and to decrease susceptibility to human phagocytic immune cells when expressed (42, 43). Spa and the Staphylococcal binding immunoglobulin protein Sbi have similar effects and functions, as they both bind the F_c region of IgG immunoglobulins and contribute to inflammatory response. However, SpaA is covalently anchored to the cell wall, while Sbi is not (43, 44). Conserved virulence factor C, encoded by *cvfC*, is instrumental in the production of hemolysin in *S. aureus*. Without any of the three genes *cvfABC*, hemolysin production is decreased in that mutant, as is overall virulence (45). Hemolysin is an exotoxin that binds to host cells without the use of receptors and creates a pore resulting in cell leakage. Ions and nutrients are lost through the membrane, which can be lethal for the cell (46). The direct association between CvfC and hemolysin production is not understood. The final virulence factor under discussion, SdrD, has roles in immune evasion and adhesion of *S. aureus.* SdrD has been shown to increase survivability of the bacteria in blood, which contributes to occurrences of *S. aureus* bacteremia in mice (44, 47). Specifically, the protein helps bacteria survive in the presence of neutrophils, and contributes to neutrophil death through unknown mechanisms or receptors (47).

The binding of IgG by Protein A and staphylococcal binding immunoglobulin protein as well as the action of SdrD all help *S.* aureus evade phagocytosis. CvfC contributes to virulence through involvement in hemolysin productions. The reduced concentrations of all of these is likely due to the fact that these cells are not facing any immune challenge. With no need for virulence proteins to infect a host for nutrients, decreasing these proteins is likely part of the strategy to conserve energy and reduce unneeded production.

Discussion

With carriage of *S. aureus* so high, and the presence of MRSA increasing in both nosocomial and community settings, understanding the effect of ABHR as a selective pressure on the bacteria is gaining importance. Through isolation of cells from 12% ethanol, the Gustafson laboratory has proven that development of ethanol reduced susceptibility SH1000 mutants via selection alcohol-based hand rubs is possible. As these isolates clearly differed in phenotype from SH1000, proteomic analysis revealed major differences in protein expression. SH123 and SH124 were isolated from the ethanol passaging process, which resulted in the small colony phenotype. This process led to changes in metabolism that correlate with a cell just trying to survive. Virulence factors are decreased in concentration. This indicates that the cells are not dedicating as much energy to infecting a host, especially in an environment where defense against a host immune system is not needed. Purine biosynthesis being reduced also reflects the reduced needs of these cells. In a slower growing cell, less chemical energy is required and the cell can conserve energy by not producing as much ATP as we see through downregulation in both purine salvage and synthesis pathway (12). The most interesting alteration to the bacterial proteome is that of the iron metabolism. Despite the reduced concentrations of proteins for other major metabolic areas, iron acquisition proteins are highly increased in SH123 and SH124 compared to SH1000. Staphyloferrin B production is most strikingly increased, with all but two associated biosynthesis proteins showing increased concentrations in the mutants. Staphyloferrin A biosynthesis and iron active transport proteins are also highly increased (12). The cause of increased cellular demand for iron is as of yet unconfirmed, as is its correlation to the small colony phenotype. However, the hypothesized connection of increased iron metabolism to increased concentrations of autolysis proteins seems likely. The functions of the autolysin proteins in question seem to be

able to degrade the cell wall in a way that allows cellular contents to escape, though further study is needed (18, 22). If this is the case, we would expect further research to find increased rates of autolysis in these mutants, and increased growth and success of mutant cells provided supplemental iron.

Future Research

Growth with Supplemental Iron

Since mutants SH123 and SH124 are demonstrating apparent iron starvation, the Gustafson lab found it important that the effect of supplemental iron be tested. If iron starvation is the underlying cause of the less-than-optimal small colony phenotype, we would expect that iron supplementation would result in increased growth of the isolated mutants.

Since it has been established that Staphyloferrins are able to steal iron from proteins including hemoglobin, simple blood plates should be a reasonable test of iron supplementation. The hemoglobin within the red blood cells will act as the additional iron source. When grown on blood plates, the expected result should not only include increased growth but also larger zones of hemolysis in the mutants compared to parent SH1000. This would demonstrate that additional staphyloferrins are being produced as demonstrated in our proteomic data, and are being put to use by harvesting iron from present hemoglobin in the media. The decrease in concentration of cvfC in the mutants may complicate this process as hemolysis may be downregulated. If this is the case a different assay may be more appropriate.

Growth with Supplemental Purines

SH123 and SH124 also show decreased concentrations of purine biosynthetic proteins, which is likely correlated with the slow growth of the small colony phenotype. If the two issues

are linked, one would reasonably suspect that purine supplementation would lead to increased growth and colony size in the mutants. Torres et al. (2019) discussed that in small colony SH1000 mutant SH1000-TTORS-1, reduced growth and altered metabolism were likely linked to the reduced DNA replication and reduced purines (15).

In addition, fatty acid biosynthesis also seemed to be impaired in SH1000-TTORS-1, which is comparable to the likely impairment in purine biosynthesis seen in Ethanol reduced susceptibility mutants SH123 and SH124. When supplemental fatty acids were provided to the SH1000-TTORS-1 mutant by way of tween-80, colony size increased (15). By the same token, it is expected that SH123 and SH124 purine supplementation would lead to similarly increased colony size and growth.

Acknowledgements

I would like to thank my Thesis Mentor, Dr. John Gustafson, as well as my second reader, Dr. Patricia Canaan, for supporting both myself and my research throughout my degree. Their contributions to the completion of this thesis is only part of what they have done over the three years I have spent with them. Additionally, I would like to thank Dr. Richard Frohock and the Honor's College for continuously checking on my progress and ensuring I always had what I needed in my pursuit of an Honor's degree, even on a tight accelerated schedule. Even with the extremely trying and complicated environment of living through the Covid-19 pandemic, the Honor's college has been extra flexible to aid students finishing their theses.

Outside of Oklahoma State University, I would like to thank my parents and my fiancé for their constant encouragement as I struggled with finishing this project. Even when lab work did not go according to plan and extenuating circumstances prevented me from repeating experiments and left me doubting what would happen to every aspect of my schoolwork, they were always there telling me I would get through it as long as I did not give up.

References

1. Graham PL, 3rd, Lin SX, Larson EL. 2006. A U.S. population-based survey of Staphylococcus aureus colonization. Ann Intern Med **144:**318-325.
2. Kourtis AP, Hatfield K, Baggs J, Mu Y, See I, Epson E, Nadle J, Kainer MA, Dumyati G, Petit S. 2019. Vital signs: epidemiology and recent trends in methicillin-resistant and in methicillin-susceptible Staphylococcus aureus bloodstream infections—United States. Morbidity and Mortality Weekly Report. **68**(9)**:**214.
3. Kochanek KD, Murphy SL, Xu J, Arias E. 2019. Deaths: Final Data for 2017. Division of Vital Statistics, Center for Disese Control.
4. Chambers HF, DeLeo FR. 2009. Waves of resistance: Staphylococcus aureus in the antibiotic era. Nature Reviews Microbiology **7:**629-641.
5. McDonnell G, Russell AD. 1999. Antiseptics and disinfectants: activity, action, and resistance. Clinical microbiology reviews **12:**147-179.
6. Earl ML, Jackson MM, Rickman LS. 2001. Improved rates of compliance with hand antisepsis guidelines: a three phase observational study. The American journal of nursing **101:**26-33.
7. Allegranzi B, Pittet D. 2009. Role of hand hygiene in healthcare-associated infection prevention. Journal of hospital infection **73:**305-315.
8. Torres NJ, Peterson WE, Gustafson JE. Ethanol Selects for Staphylococcus aureus Small Colony Variant Mutants Demonstrating Reduced Susceptibility to Ethanol. Oklahoma State Universuty.
9. Pidot SJ, Gao W, Buultjens AH, Monk IR, Guerillot R, Carter GP, Lee JY, Lam MM, Grayson ML, Ballard SA. 2018. Increasing tolerance of hospital Enterococcus faecium to handwash alcohols. Science Translational Medicine **10:**eaar6115.
10. Torres NJ, Peterson WE, Gustafson JE. Ethanol Selection in vitro & Gradient Plate Analysis, Colony Size, and Growth.
11. Proctor RA, Kriegeskorte A, Kahl BC, Becker K, Löffler B, Peters G. 2014. Staphylococcus aureus small colony variants (SCVs): a road map for the metabolic pathways involved in persistent infections. Frontiers in cellular and infection microbiology **4:**99.
12. Gustafson JE. SH1000 Proteomics Data.
13. Pando JM, Pfeltz RF, Cuaron JA, Nagarajan V, Mishra MN, Torres NJ, Elasri MO, Wilkinson BJ, Gustafson JE. 2017. Ethanol-induced stress response of Staphylococcus aureus. Canadian journal of microbiology **63:**745-757.
14. Torres NJ, Peterson WE, Gustafson JE. Ethanol Selects for Staphylococcus aureus Small Colony Variant Mutants Demonstrating Reduced Susceptibility to Ethanol., p 16. Department of Biochemistry and Molecular Biology.
15. Torres NJ, Hartson SD, Rogers J, Gustafson JE. 2019. Proteomic and Metabolomic Analyses of a Tea-Tree Oil-Selected Staphylococcus aureus Small Colony Variant. Antibiotics **8:**248.
16. Voruganti S, LaCroix JC, Rogers CN, Rogers J, Matts RL, Hartson SD. 2013. The Anticancer Drug AUY922 Generates a Proteomics Fingerprint That Is Highly Conserved among Structurally Diverse Hsp90 Inhibitors. Journal of Proteome Research **12:**3697-3706.
17. Bose JL, Lehman MK, Fey PD, Bayles KW. 2012. Contribution of the Staphylococcus aureus Atl AM and GL murein hydrolase activities in cell division, autolysis, and biofilm formation. PloS one **7**.
18. Stapleton MR, Horsburgh MJ, Hayhurst EJ, Wright L, Jonsson I-M, Tarkowski A, Kokai-Kun JF, Mond JJ, Foster SJ. 2007. Characterization of IsaA and SceD, Two Putative Lytic Transglycosylases of Staphylococcus aureus. Journal of Bacteriology **189:**7316-7325.
19. Delaune A, Poupel O, Mallet A, Coic Y-M, Msadek T, Dubrac S. 2011. Peptidoglycan Crosslinking Relaxation Plays an Important Role in Staphylococcus aureus WalKR-Dependent Cell Viability. PLOS ONE **6:**e17054.
20. Szklarczyk D, Gable AL, Lyon D, Junge A, Wyder S, Huerta-Cepas J, Simonovic M, Doncheva NT, Morris JH, Bork P, Jensen LJ, Mering CV. 2019. STRING v11: protein-protein association networks with increased coverage, supporting functional discovery in genome-wide

experimental datasets. Nucleic Acids Res **47:**D607-d613.
21. **Lioliou E, Fechter P, Caldelari I, Jester BC, Dubrac S, Helfer A-C, Boisset S, Vandenesch F, Romby P, Geissmann T.** 2016. Various checkpoints prevent the synthesis of Staphylococcus aureus peptidoglycan hydrolase LytM in the stationary growth phase. RNA biology **13:**427-440.
22. **Zoll S, Pätzold B, Schlag M, Götz F, Kalbacher H, Stehle T.** 2010. Structural Basis of Cell Wall Cleavage by a Staphylococcal Autolysin. PLOS Pathogens **6:**e1000807.
23. **Ponka P.** 1999. Cellular iron metabolism. Kidney International **55:**S2-S11.
24. **Puig S, Ramos-Alonso L, Romero AM, Martínez-Pastor MT.** 2017. The elemental role of iron in DNA synthesis and repair. Metallomics **9:**1483-1500.
25. **Yost FJ, Fridovich I.** 1973. An Iron-containing Superoxide Dismutase from Escherichia coli. Journal of Biological Chemistry **248:**4905-4908.
26. **Beasley FC, Marolda CL, Cheung J, Buac S, Heinrichs DE.** 2011. Staphylococcus aureus Transporters Hts, Sir, and Sst Capture Iron Liberated from Human Transferrin by Staphyloferrin A, Staphyloferrin B, and Catecholamine Stress Hormones, Respectively, and Contribute to Virulence. Infection and Immunity **79:**2345.
27. **Haag H, Fiedler H-P, Meiwes J, Drechsel H, Jung G, Zähner H.** 1994. Isolation and biological characterization of staphyloferrin B, a compound with siderophore activity from staphylococci. FEMS Microbiology Letters **115:**125-130.
28. **Meiwes J, Fiedler H-P, Haag H, Zähner H, Konetschny-Rapp S, Jung G.** 1990. Isolation and characterization of staphyloferrin A, a compound with siderophore activity from Staphylococcus hyicus DSM 20459. FEMS Microbiology Letters **67:**201-205.
29. **Trivier D, Courcol RJ.** 1996. Iron depletion and virulence in Staphylococcus aureus. FEMS Microbiology Letters **141:**117-127.
30. **Cotton JL, Tao J, Balibar CJ.** 2009. Identification and Characterization of the Staphylococcus aureus Gene Cluster Coding for Staphyloferrin A. Biochemistry **48:**1025-1035.
31. **Grigg JC, Cheung J, Heinrichs DE, Murphy MEP.** 2010. Specificity of Staphyloferrin B Recognition by the SirA Receptor from Staphylococcus aureus. Journal of Biological Chemistry **285:**34579-34588.
32. **Cheung J, Beasley FC, Liu S, Lajoie GA, Heinrichs DE.** 2009. Molecular characterization of staphyloferrin B biosynthesis in Staphylococcus aureus. Mol Microbiol **74:**594-608.
33. **Sebulsky MT, Hohnstein D, Hunter MD, Heinrichs DE.** 2000. Identification and characterization of a membrane permease involved in iron-hydroxamate transport in Staphylococcus aureus. Journal of bacteriology **182:**4394-4400.
34. **Anonymous.** 2020. FecCD iron compound ABC transporter, permease family protein, February 26, 2020 ed. UniProt, UniProtKB.
35. **Cao H, Wei D, Yang Y, Shang Y, Li G, Zhou Y, Ma Q, Xu Y.** 2017. Systems-level understanding of ethanol-induced stresses and adaptation in E. coli. Scientific Reports **7:**44150.
36. **Anonymous.** UniProtKB - P39451 (ADHP_ECOLI).
37. **Wetherell M.** 1998. Molecular & physical characterization of threonine dehydrogenase from Serratia marcescens.
38. **Anonymous.** UniProtKB - Q6GH69 (GUAC_STAAR).
39. **Martinelli LK, Ducati RG, Rosado LA, Breda A, Selbach BP, Santos DS, Basso LA.** 2011. Recombinant Escherichia coli GMP reductase: kinetic, catalytic and chemical mechanisms, and thermodynamics of enzyme-ligand binary complex formation. Mol Biosyst **7:**1289-1305.
40. **Zhang Y, Morar M, Ealick SE.** 2008. Structural biology of the purine biosynthetic pathway. Cellular and Molecular Life Sciences **65:**3699-3724.
41. **Bronner S, Monteil H, Prévost G.** 2004. Regulation of virulence determinants in Staphylococcus aureus: complexity and applications. FEMS microbiology reviews **28:**183-200.
42. **Palmqvist N, Foster T, Tarkowski A, Josefsson E.** 2002. Protein A is a virulence factor in Staphylococcus aureus arthritis and septic death. Microbial pathogenesis **33:**239-249.
43. **Gonzalez CD, Ledo C, Giai C, Garófalo A, Gómez MI.** 2015. The Sbi Protein Contributes to Staphylococcus aureus Inflammatory Response during Systemic Infection. PloS one **10:**e0131879-e0131879.
44. **Foster TJ, Geoghegan JA, Ganesh VK, Höök M.** 2014. Adhesion, invasion and evasion: the

many functions of the surface proteins of Staphylococcus aureus. Nature Reviews Microbiology **12:**49-62.

45. **Kaito C, Kurokawa K, Matsumoto Y, Terao Y, Kawabata S, Hamada S, Sekimizu K.** 2005. Silkworm pathogenic bacteria infection model for identification of novel virulence genes. Molecular Microbiology **56:**934-944.

46. **Elliott SJ, Srinivas S, Albert MJ, Alam K, Robins-Browne RM, Gunzburg ST, Mee BJ, Chang BJ.** 1998. Characterization of the Roles of Hemolysin and Other Toxins in Enteropathy Caused by Alpha-Hemolytic Escherichia coli Linked to Human Diarrhea. Infection and Immunity **66:**2040-2051.

47. **Askarian F, Uchiyama S, Valderrama JA, Ajayi C, Sollid JUE, van Sorge NM, Nizet V, van Strijp JAG, Johannessen M.** 2017. Serine-Aspartate Repeat Protein D Increases Staphylococcus Virulence and Survival in Blood. Infection and Immunity **85:**e00559-00516.